

Transport properties of silicon implanted with bismuth

E. Abramof* and A. Ferreira da Silva†

Instituto Nacional de Pesquisas Espaciais-INPE, Laboratório Associado de Sensores e Materiais-LAS, Caixa Postal 515, 12201-970 São José dos Campos, São Paulo, Brazil

Bo E. Sernelius

Department of Physics, Linköping University, S-581 83 Linköping, Sweden

J. P. de Souza and H. Boudinov

Instituto de Física UFRGS, 91501-970 Porto Alegre, Rio Grande do Sul, Brazil

(Received 7 May 1996; revised manuscript received 20 October 1996)

The Hall effect and resistivity of Si:Bi with donor concentration varying from 3.0×10^{17} to 1.4×10^{20} cm^{-3} were measured from room temperature down to 13 K. The samples were prepared by Bi^+ implantation in Van der Pauw structures delineated in Si chips. The measured resistivities were compared with the ones calculated by a generalized Drude approach at similar temperatures and doping concentration, presenting fairly good agreement. The critical impurity concentration N_c of the metal-nonmetal transition was measured to be around 2×10^{19} cm^{-3} . The critical concentration N_c was calculated by comparing the ionization energy of the insulating phase with the total energy of the metallic phase. This value of N_c agreed very well with the one obtained experimentally and the values estimated from other theoretical approaches. [S0163-1829(97)01612-3]

INTRODUCTION

The interest in the experimental and the theoretical investigation of the electronic properties of n -doped silicon has recently increased.¹⁻²⁰ The importance of disorder and correlation effects around the impurity critical concentration N_c for the metal-nonmetal (MNM) transition is still the subject of many investigation.¹⁻¹⁰

Bismuth-doped silicon (Si:Bi), which has received much less attention than other donors in Si, has a larger ionization energy (smaller effective Bohr radius) and consequently higher critical concentration N_c when compared to the other group-V donors (P, As, and Sb).¹¹ These characteristics make the Si:Bi system very appropriate for the theoretical modeling of the transport properties from the insulating to the metallic phase, as well as for the investigation of the different mechanisms responsible for the MNM transition.

In this work, the primary emphasis will be on the resistivity and Hall effect measurements in Si:Bi, from room temperature down to 13 K, with variation of the impurity concentration in the insulator to metallic range. The measured samples were prepared by Bi^+ implantation in Van der Pauw structures delineated in Si chips. The band conduction and impurity conduction activation energies were obtained from the slopes of the two branches of the resistivity curves.

The resistivities obtained experimentally are compared with the ones calculated from a recently proposed generalized Drude approach (GDA) at similar temperatures and doping regimes. For the resistivity calculation, we start from a frequency-dependent general expression for a polar semiconductor, reducing it to a nonpolar one in the static regime considering the effects of scattering by a random distribution of Coulomb impurities. The value of the critical concentration N_c is obtained by comparing the ionization energy in the insulating phase E_I with the total energy in the metallic

phase E_T . The ionization energy E_I is calculated using the dielectric function model with a Lorentz-Lorenz correction. This value of N_c obtained in such a general mode is compared with the ones estimated from other theoretical approaches and the experimental value determined during this work.

EXPERIMENT

We use p -type, (100)-oriented Si wafers with resistivity in the range 16–25 Ω cm. Bismuth was implanted at room temperature in Van der Pauw structures²¹ with contact areas presenting low sheet resistance ($< 20 \Omega/\square$, phosphorous doped). Five implantation with energies of 360, 200, 120, 70, and 35 keV were accumulated in each sample with proper doses to result in a plateaulike profile of Bi from the surface to the depth of 0.12 μm with $\sim 5\%$ deviation, according to TRIM code simulation.²²

The implanted Bi doses were 2.5×10^{15} cm^{-2} (at 360 keV), 1.4×10^{15} cm^{-2} (at 200 keV), 8×10^{14} cm^{-2} (at 120 keV), 7×10^{14} cm^{-2} (at 70 keV), and 5×10^{14} cm^{-2} (at 35 keV) in order to achieve a Bi concentration of 5×10^{20} cm^{-3} . The doses in the other samples were scaled to this sample with 5×10^{20} cm^{-3} , according to the ratio of the desired Bi concentration. Samples with implanted Bi concentration from 5×10^{17} to 5×10^{20} cm^{-3} were prepared.

The damage annealing and the electrical activation of Bi were performed at 600 $^\circ\text{C}$ for 30 min in inert atmosphere in a halogen lamp furnace. For samples with Bi concentration less than 1×10^{19} cm^{-3} , a second annealing step was performed at 900 $^\circ\text{C}$ for 60 s. The annealing process is described in detail elsewhere.^{2,23}

The as-implanted and annealed samples were analyzed by Rutherford backscattering spectrometry using 760-keV He^{2+} beam in random and in (100)-aligned (RBS/C) incidence di-

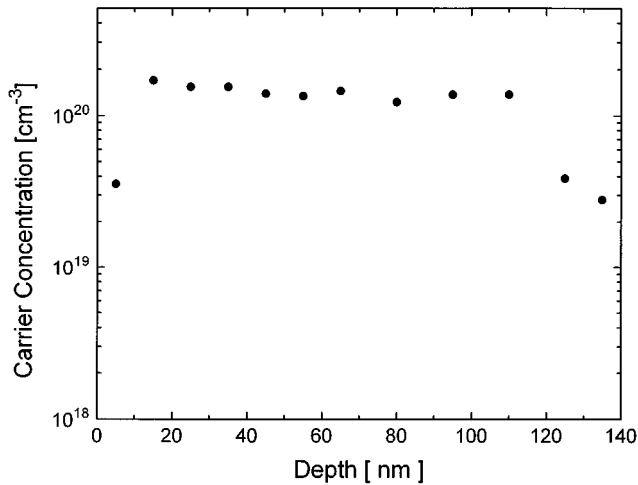


FIG. 1. Carrier depth profile of a sample implanted with the highest Bi dose ($5.9 \times 10^{15} \text{ cm}^{-2}$) after annealing at 600°C for 30 min.

rections. The carrier concentration depth distribution was obtained in the annealed Van der Pauw devices via sequential anodic oxidation and oxide stripping followed by sheet resistance and Hall effect measurements.

The electrical measurements were performed in an automated Keithley 180A Hall effect system. The Van der Pauw Si:Bi samples were mounted in a He closed-cycle cryostat that allowed Hall effect and resistivity measurements from room temperature down to 13 K. The measured electron concentration of the prepared samples at 290 K ranged from 3.0×10^{17} to $1.4 \times 10^{20} \text{ cm}^{-3}$; these values are considered in this work as the donor impurity concentration N_d of the samples.

RESULTS

RBS/C analysis revealed that the as-implanted sample with the lower Bi dose (total dose of $5.9 \times 10^{12} \text{ cm}^{-2}$) is crystalline with defect concentration level of 10% in a layer extending from the surface up to the depth of $0.12 \mu\text{m}$. In other samples the Bi-implanted layer was rendered amorphous.

The layer implanted to the highest Bi dose (total dose of $5.9 \times 10^{15} \text{ cm}^{-2}$) was epitaxially recrystallized during annealing, presenting a residual defect concentration below the detection level of our RBS/C analysis (less than 1%). However, a highly defective layer (thickness of 20 nm) remained at the sample surface. In the other samples the residual defect concentration after annealing is below the detection level along all the depth.

Figure 1 shows the carrier concentration depth profile of the sample implanted with the highest total Bi dose ($5.9 \times 10^{15} \text{ cm}^{-2}$) after annealing. The profile is flat topped, extending from a depth of 10 nm up to 120 nm, with an average concentration of $1.4 \times 10^{20} \text{ cm}^{-3}$. This value represents an electrical activation of about 28% of the implanted Bi atoms. It is interesting to point out that this activated concentration is three orders of magnitude higher than the solid solubility of Bi in Si at 1100°C .²⁴ Such a highly activated Bi concentration has been previously observed to form

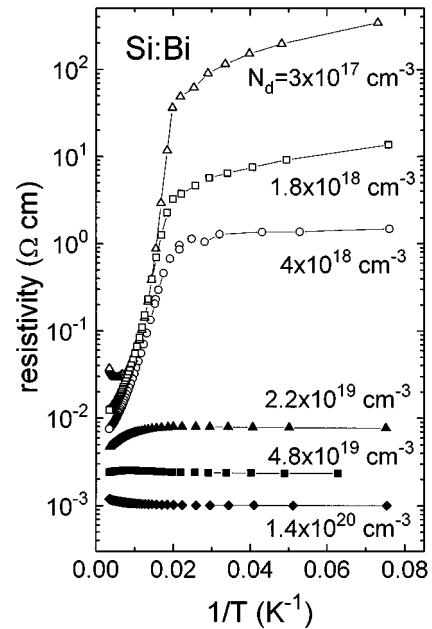


FIG. 2. Electrical resistivity of Si:Bi with different donor impurity concentration N_d versus the inverse temperature.

during solid-phase epitaxial regrowth of an amorphized layer and presents metastability during annealing.²³

Figures 2 and 3 show the electrical resistivity and Hall coefficient of the Si:Bi samples with different donor impurity concentration N_d as a function of temperature. The metallic character of the samples with N_d higher than $2 \times 10^{19} \text{ cm}^{-3}$ (three curves in the bottom part of both graphs) is evidenced by the temperature-independent values of both resistivity and Hall coefficient through the whole temperature range investigated.

For samples with Bi donor concentration less than 2×10^{19}

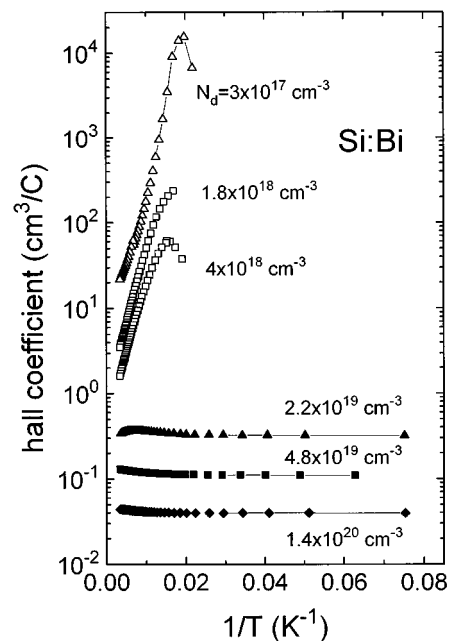


FIG. 3. Temperature dependence of the Hall coefficient of Si:Bi samples with different donor concentration N_d .

TABLE I. Band conduction activation energy E_1 and the impurity conduction activation energy E_2 for Si:Bi.

| N_d (cm^{-3}) | E_1 (10^{-3} eV) | E_2 (10^{-3} eV) |
|----------------------------|-----------------------|-----------------------|
| 3.0×10^{17} | 70.6 | 2.2 |
| 1.8×10^{18} | 40.2 | 1.5 |
| 4.0×10^{18} | 31.6 | 0.3 |

cm^{-3} , the large enhancement in the resistivity and Hall coefficient as the temperature decreases, due to the reduction of free electrons in the conduction band, demonstrates the semiconductor properties of the Si:Bi samples in this range of N_d . At the temperature where the impurity conduction starts to replace the band conduction transport, the Hall coefficient curves of these samples show a maximum and the resistivity curves change their slopes drastically. As shown in Fig. 3, the maximum in the Hall coefficient curves shifts to higher temperatures as N_d increases.

The band conduction activation energy E_1 and the impurity conduction activation energy E_2 calculated from the slopes of the two branches of the $\log_{10} \rho$ vs $1/T$ curves are shown in Table I for the three semiconducting samples. The value $E_1 = 71$ meV, considered as the donor ionization energy of Bi in Si,¹¹ was found only for the most diluted sample with $N_d = 3 \times 10^{17} \text{ cm}^{-3}$. As the donor concentration N_d increases towards the critical concentration N_c , the measured activation energy E_1 decreases its value, as expected in such a MNM transition.²⁵ The values of E_2 shown in Table I were calculated in the part of the curve where $1/T$ is higher than 0.03 K^{-1} , as only at these temperatures the slopes approach a constant value. These values are very small, showing an almost metallic impurity conduction. This fact was also observed for GaAs:Mn, which is an acceptor with almost the same ionization energy of Bi in Si.²⁶ The activation energy E_2 also decreases as N_d increases, showing the same behavior as for E_1 .

Figure 4(a) shows the resistivity dependence of Si:Bi on the donor impurity concentration N_d at different temperatures. We can observe that all the curves ρ vs N_d for different temperatures merge together to one critical point. This plot indicates clearly that the critical impurity concentration N_c for the metal-nonmetal transition is around $2 \times 10^{19} \text{ cm}^{-3}$ for silicon doped with bismuth. Figure 4(b) shows the theoretical resistivity of Si:Bi calculated from the generalized Drude approach with the same donor concentration and temperatures of Fig. 4(a). The calculations using the GDA method to determine the resistivity and the theoretical determination of the critical concentration of Si:Bi are described in the next section.

THEORY AND DISCUSSION

In order to calculate the dependence of the resistivity on temperature and impurity concentration, we use the generalized Drude approach. In the GDA, one starts from a generalized Drude expression for the dynamical conductivity^{20,27,28}

$$\sigma(\omega) = \frac{Ne^2}{m^*} \frac{1}{1/\tau(\omega) - i\omega}, \quad (1)$$

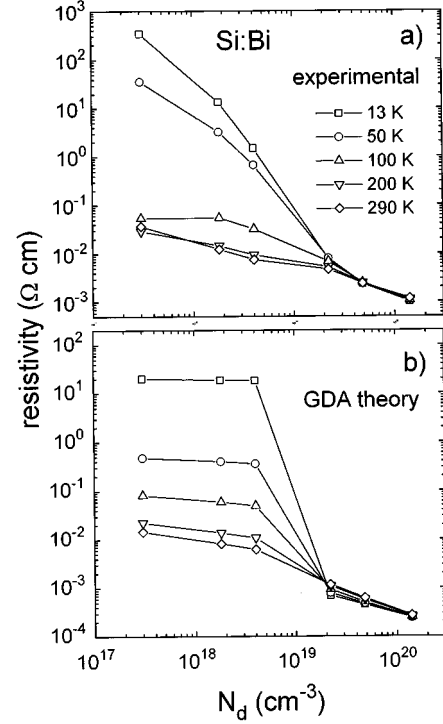


FIG. 4. Si:Bi resistivity as a function of the donor concentration N_d (a) measured at different temperatures and (b) calculated by the generalized Drude approach at the same N_d values and temperatures.

with a generalized complex-valued and frequency-dependent relaxation time $\tau(\omega)$. The expression found for $\tau(\omega)$ is valid for all frequencies, in particular for zero frequency, which is what we are interested in here. The net effect of the GDA is derived in the more general case of a polar semiconductor.^{27,29} The resistivity is then obtained as $1/\sigma$ and is found to be²⁷

$$\rho(\omega) = \frac{-im^*\omega}{N_d e^2} - \frac{i2}{3\pi N_d \omega} \times \int_0^\infty q^2 \frac{[\alpha(q, \omega) - \alpha(q, 0)][\epsilon_L(q, \omega) + \alpha(q, 0)]}{\epsilon_T^2(q, 0)\epsilon_T(q, \omega)} dq. \quad (2)$$

In the above expression, N_d is the donor impurity concentration, e is the electric charge, m^* is the effective mass, α is the polarizability from the carriers, ϵ_L is the lattice dielectric function, and ϵ_T is the total dielectric function.²⁷

For frequency independent ϵ_L and no phonon polarizability, Eq. (2) reduces to the expression for a nonpolar semiconductor^{2,18}

$$\rho(\omega) = \frac{-im^*\omega}{N_d e^2} + \frac{i2}{3\pi N_d \omega} \int_0^\infty q^2 \left[\frac{1}{\epsilon_T(q, \omega)} - \frac{1}{\epsilon_T(q, 0)} \right] dq, \quad (3)$$

which is identical to the result obtained in the so-called energy loss method.³⁰ We have assumed a random distribution of Coulomb impurities.

The dielectric function ϵ_T is given by

$$\varepsilon_T(q, \omega) = \varepsilon + v\alpha_1(q, \omega) + iv\alpha_2(q, \omega), \quad (4)$$

where ε is the dielectric constant for Si and α_1 and α_2 are the real and imaginary parts of the polarizabilities from one of the v valleys of dopant carriers. The number of valleys is 6 in Si, and these functions are temperature dependent.

We are interested in the static resistivity, which can be written as

$$\alpha_2(Q, W) = -\frac{m^*e^2}{8\hbar k_F Q^3 B} \left[\ln \left(\frac{\cosh\{B[W + (Q^2 + W^2/Q^2 - M)/2]\}}{\cosh\{B[W - (Q^2 + W^2/Q^2 - M)/2]\}} \right) - 2BW \right], \quad (6)$$

where we have introduced the dimensionless variables $Q = q/2k_F$, $W = \hbar\omega/4E_F$, $B = \beta E_F$, and $M = \mu/E_F$. The quantity k_F is the Fermi wave number, E_F is the Fermi energy, μ is the chemical potential, and $\beta = 1/K_B T$, where K_B is the Boltzmann constant. The real part can be obtained from the imaginary part through the Kramers-Kronig dispersion relation.

The resistivity is reduced to

$$\rho(0) = \frac{2v(m^*e)^2}{3\pi N_d \hbar^3 k_F} \int_0^\infty \frac{\{1 - \tanh[0.5B(Q^2 - M)]\}}{Q[\varepsilon + v\alpha_1(Q, 0)]} dQ. \quad (7)$$

The temperature variation of μ is obtained from the implicit expression^{18,32}

$$B^{3/2} = \int_0^U \frac{3y}{1-y^2} \{A + \ln[(1-y^2)/y^2]\}^{1/2} dy, \quad (8)$$

where $U = (1 + e^{-A})^{-1/2}$ and $A = BM = \mu\beta$. For a given A one obtains B . This means that a relation between A and B is found.

The calculated resistivity of Si:Bi as a function of impurity concentration and temperature obtained using the procedure described above is presented in Fig. 4(b). For comparison, the resistivities of Si:Bi were calculated at the same donor concentration and temperatures of the measured samples [Fig. 4(a)]. In both graphs, the resistivity at different temperatures converge to one common value at the same donor concentration around $2 \times 10^{19} \text{ cm}^{-3}$, which is determined to be the critical concentration N_c for the MNM transition in Si:Bi. Despite the differences in the absolute resistivity values, both measured and calculated ρ vs N_d curves presented similar forms. However, a qualitative difference between the theoretical and experimental curves is observed for the low-density region at low temperatures. The theoretical curves show a much weaker density dependence than the experimental ones. This is probably due to the neglect of multiple scattering in the theory. Multiple scattering, which leads to an enhancement of the resistivity, becomes of increasing importance at lower carrier concentration and temperature.

To determine the impurity critical concentration for the MNM transition we use a model with one localized donor level below the conduction band. The carriers are distributed

$$\rho(0) = \frac{16\hbar k_F^3 v}{12\pi N_d E_F} \int_0^\infty Q^2 \frac{\left. \frac{\partial \alpha_2(Q, W)}{\partial W} \right|_{W=0}}{[\varepsilon + v\alpha_1(Q, 0)]^2} dQ. \quad (5)$$

The imaginary part can be obtained analytically in the random-phase approximation.³¹ It is given by

throughout this level and the continuum states according to the Fermi-Dirac distribution function. We compare the energy in the insulating phase, the ionization energy E_I , with the energy per electron in the metallic phase E_T . The later one includes the kinetic energy, the exchange and correlation energies, and the electron-ion interaction energy. The reader should refer to Refs. 33 and 34 for more details about the derivation of this total energy.

The ionization energy E_I is determined using the Lorentz expression for the dielectric function with the Lorentz-Lorentz correction. The dielectric function for silicon plus unionized donors is

$$\varepsilon(\omega) = 1 + \frac{4\pi N_u \alpha_d \omega_0^2}{\omega_0^2 - \omega^2 - i\Gamma\omega} + 4\pi N_h \alpha_h}{1 - \frac{1}{3} \left(\frac{4\pi N_u \alpha_d \omega_0^2}{\omega_0^2 - \omega^2 - i\Gamma\omega} + 4\pi N_h \alpha_h \right)}, \quad (9)$$

where N_u is the density of unionized donors, N_h is the contribution of the host charge density, $E_0 = \hbar\omega_0$ is the ionization energy for a single donor, and α_d and α_h are the contribution from the static polarizabilities for the unionized donors and host, respectively.

Developing the expression for $\varepsilon(\omega)$, the ionization frequency ω_I can be identified as

$$\omega_I = \omega_0 \left(1 - \frac{4\pi(\kappa + 2)N_u \alpha_d}{9} \right)^{1/2}, \quad (10)$$

where

$$\kappa = 1 + \frac{4\pi N_h \alpha_h}{1 - \frac{1}{3}(4\pi N_h \alpha_h)}. \quad (11)$$

The ionization energy $E_I = \hbar\omega_I$ as a function of N_u is written as

$$E_I = E_0 \left[1 - \frac{\pi(\kappa + 2)N_u}{4} \left(\frac{e^2}{\kappa E_0} \right)^3 \right]^{1/2}, \quad (12)$$

where we have used $\alpha_d = 9/2a_d^3$ and the Bohr radius for the donor $a_d = e^2/2\kappa E_0$, expressed as a function of the ionization energy for an isolated donor E_0 . The density of unionized donors N_u is related to the donor impurity concentration

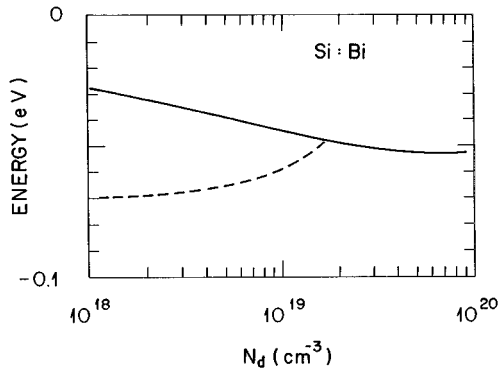


FIG. 5. Ionization energy of the insulating phase E_I (dashed curve) and the energy of the metallic phase E_T (solid curve) of Si:Bi versus the donor concentration N_d .

N_d according to the Fermi-Dirac distribution with the chemical potential μ determined by Eq. (8).

The ionization energy in the insulating phase E_I for Si:Bi was calculated using Eq. (12) and assuming the experimental value of 71 meV for E_0 . This value of 71 meV is considered to be the donor ionization energy of Bi in Si and was measured in this work for the most diluted sample (first E_I value in Table I). Figure 5 shows the ionization energy of the insulating phase E_I (dashed curve) and the energy of the metallic phase E_T (solid curve) of Si:Bi as a function of the impurity donor concentration N_d . At the point where these energies cross, we obtain the critical concentration N_c for the MNM transition. The value N_c obtained in the crossing point is $1.69 \times 10^{19} \text{ cm}^{-3}$.

The critical concentration N_c can be obtained in a simpler way instead of the complex method of calculating and com-

paring E_I with E_T by just finding the donor concentration where E_I vanishes in Eq. (12), replacing κ by the dielectric constant ϵ and assuming $N_u = N_d$. We found $N_c = 1.69 \times 10^{19}$ and $1.88 \times 10^{19} \text{ cm}^{-3}$ for $\epsilon = 11.4$ and 12.0 , respectively, with the same $E_0 = 71 \text{ meV}$ of Bi in Si. Both values of N_c are very close to a value estimated previously,¹¹ i.e., $N_c = 1.8 \times 10^{19} \text{ cm}^{-3}$. These values of the impurity critical concentration N_c of Si:Bi determined theoretically by different methods agree very well with the value determined experimentally in this work.

CONCLUSION

In summary, the resistivity and Hall effect of silicon implanted with bismuth with impurity concentrations in the insulator to metallic phase were investigated experimentally as a function of temperature. The generalized Drude approach used to calculate the concentration and temperature-dependent resistivity worked well for the Si:Bi system, presenting fairly good agreement with the experimental results. The model, in which the ionization energy of the insulating phase is compared with the total energy in the metallic phase, applied to determine the impurity critical concentration for the MNM transition of Si:Bi presented good results when compared with the experimental value obtained here and the estimated values derived by other theoretical approaches.

ACKNOWLEDGMENTS

The authors acknowledge FAPESP (Project No. 94/1798-3) and the Brazilian Research Council CNPq for the financial support. We also thank Professors M. Sarachik and H. v. Löhneysen for very helpful correspondence.

*Electronic address: abramof@las.inpe.br

†Also at Department of Physics, Linköping University, S581 83 Linköping, Sweden.

¹S. Bogdanovich, Peihua Dai, M. P. Sarachik, and V. Dobrosavljevic, *Phys. Rev. Lett.* **74**, 2543 (1995).

²A. Ferreira da Silva, Bo E. Sernelius, J. P. de Souza, and H. Boudinov, *J. Appl. Phys.* **79**, 3453 (1996).

³T. G. Castner, *Phys. Rev. B* **52**, 12 434 (1995).

⁴Peihua Dai, Youzhu Zhang, and M. P. Sarachik, *Phys. Rev. B* **52**, 12 439 (1995).

⁵A. Gaymann, H. P. Geserich, and H. v. Löhneysen, *Phys. Rev. B* **52**, 16 486 (1995).

⁶M. Straub, K. Kirch, and H. v. Löhneysen, *Z. Phys. B* **95**, 31 (1994).

⁷M. Hornung, A. Ruzzu, H. G. Schlager, H. Staupp, and H. v. Löhneysen, *Europhys. Lett.* **28**, 43 (1994).

⁸T. G. Castner, *Phys. Rev. Lett.* **73**, 3600 (1994).

⁹Peihua Dai, Youzhu Zhang, and M. P. Sarachik, *Phys. Rev. B* **49**, 14 039 (1994).

¹⁰D. Belitz and T. Kirkpatrick, *Rev. Mod. Phys.* **66**, 261 (1994).

¹¹A. Ferreira da Silva, *J. Appl. Phys.* **76**, 5249 (1994).

¹²A. Ferreira da Silva, *Phys. Rev. B* **50**, 11 216 (1994).

¹³A. Ferreira da Silva, *Phys. Rev. B* **48**, 1921 (1993).

¹⁴G.-J. Yi and G. F. Neumark, *Phys. Rev. B* **48**, 17 043 (1993).

¹⁵M. J. Hirsch, D. F. Holcomb, R. N. Bhatt, and M. A. Paalanen,

Phys. Rev. Lett. **68**, 1418 (1992).

¹⁶U. Thomanscheksky and D. F. Holcomb, *Phys. Rev. B* **45**, 13 356 (1992).

¹⁷Peihua Dai, Youzhu Zhang, and M. P. Sarachik, *Phys. Rev. Lett.* **66**, 1914 (1991).

¹⁸Bo E. Sernelius and E. Söderström, *J. Phys.: Condens. Matter* **3**, 1493 (1991).

¹⁹Bo E. Sernelius, *Phys. Rev. B* **43**, 7136 (1991).

²⁰Bo E. Sernelius, *Phys. Rev. B* **41**, 3060 (1990).

²¹L. J. Van der Pauw, *Philips Res. Rep.* **13**, 1 (1958).

²²J. F. Ziegler, J. P. Biersak, and U. Littmark, *The Stopping and Ranges of Ion in Solids* (Pergamon, New York, 1985), Vol. I.

²³J. P. de Souza and P. F. P. Fichtner, *J. Appl. Phys.* **74**, 119 (1993).

²⁴F. A. Trumbore, *Bell Syst. Tech. J.* **39**, 205 (1960).

²⁵H. Fritzsche, in *The Metal-Nonmetal Transition in Doped Semiconductors*, edited by L. R. Friedman and D. P. Tunstall (Scottish Universities Summer School in Physics, Edinburgh, 1979), p. 193.

²⁶D. A. Woodbury and J. S. Blakemore, *Phys. Rev. B* **8**, 3803 (1973).

²⁷Bo E. Sernelius, *Phys. Rev. B* **36**, 1080 (1987).

²⁸Bo E. Sernelius, *Phys. Rev. B* **40**, 12 438 (1989).

²⁹Bo E. Sernelius and M. Morling, *Thin Solid Films* **177**, 69 (1989).

³⁰E. Gerlach, J. Phys. C. **19**, 4585 (1986).

³¹R. Sirko and D. L. Mills, Phys. Rev. B **18**, 4373 (1978).

³²Bo. E. Sernelius, in *Shallow Impurities in Semiconductors*, Proceedings of the Third International Conference in Shallow Impurities in Semiconductors, edited by B. Monemar, IOP Conf. Proc. No. 95 (Institute of Physics and Physical Society, London,

1988), p. 137

³³K.-F. Berggren and Bo E. Sernelius, Phys. Rev. B **24**, 1971 (1981).

³⁴Bo E. Sernelius and K.-F. Berggren, Philos. Mag. B **43**, 115 (1981).